

# **Assessment of Human Emotional States by Optimizing the Electrodermal Activity Signals with Two-dimensional Representations and Machine Learning**



**Thesis submitted in partial fulfilment**

**for the Award of**

**DOCTOR OF PHILOSOPHY**

**by**

**SRIRAM KUMAR P**

**SCHOOL OF BIOMEDICAL ENGINEERING**

**INDIAN INSTITUTE OF TECHNOLOGY**

**(BANARAS HINDU UNIVERSITY)**

**VARANASI – 221 005**


ROLL NUMBER  
21021003

YEAR OF SUBMISSION  
2024

## CERTIFICATE

It is certified that the work contained in the thesis titled **Assessment of Human Emotional States by Optimizing the Electrodermal Activity Signals with Two-dimensional Representations and Machine Learning** by **Sriram Kumar P** has been carried out under my supervision and that this work has not been submitted elsewhere for a degree.

It is further certified that the student has fulfilled all the requirements of Comprehensive Examination, Candidacy and SOTA for the award of **Doctor of Philosophy**.


  
**Supervisor**  
**Dr. Jac Fredo AR**  
School of Biomedical Engineering  
Indian Institute of Technology  
(Banaras Hindu University)  
Varanasi – 221 005

**SUPERVISOR**

## DECLARATION BY THE CANDIDATE

I, **Sriram Kumar P**, certify that the work embodied in this thesis is my own bona fide work and carried out by me under the supervision of **Dr. Jac Fredo AR** from **July 2021** to **May 2024**, at the **School of Biomedical Engineering**, Indian Institute of Technology (Banaras Hindu University), Varanasi. The matter embodied in this thesis has not been submitted for the award of any other degree/diploma. I declare that I have faithfully acknowledged and given credits to the research workers wherever their works have been cited in my work in this thesis. I further declare that I have not willfully copied any other's work, paragraphs, text, data, results, *etc.*, reported in journals, books, magazines, reports, dissertations, theses, *etc.*, or available at websites and have not included them in this thesis and have not cited as my own work.

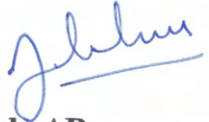
Date: May 28, 2024  
Place: Varanasi, India

  
Signature of the Student


---

## CERTIFICATE BY THE SUPERVISOR

It is certified that the above statement made by the student is correct to the best of my knowledge.

  
**Supervisor**  
**Dr. Jac Fredo AR**  
School of Biomedical Engineering  
Indian Institute of Technology  
(Banaras Hindu University)  
Varanasi – 221 005

**SUPERVISOR**

  
**Coordinator** 30.05.24  
समन्वयक/CO-ORDINATOR  
जैव चिकित्सा अभियांत्रिकी स्कूल  
SCHOOL OF BIOMEDICAL ENGG.  
भारतीय प्रौद्योगिकी संस्थान (का.हि.वि.)  
INDIAN INSTITUTE OF TECHNOLOGY (B.H.U.)  
वाराणसी-221005/VARANASI-221005

## **COPYRIGHT TRANSFER CERTIFICATE**

**Title of the Thesis:** Assessment of Human Emotional States by Optimizing the Electro-dermal Activity Signals with Two-dimensional Representations and Machine Learning

**Name of the Student:** Sriram Kumar P

## **COPYRIGHT TRANSFER**

**The undersigned hereby assigns to the Indian Institute of Technology (Banaras Hindu University), Varanasi all rights under copyright that may exist in and for the above thesis submitted for the award of the Doctor of Philosophy.**

Date: May 28, 2024  
Place: Varanasi, India

  
Signature of the Student

**Note: However, the author may reproduce or authorize others to reproduce material extracted verbatim from the thesis or derivative of the thesis for author's personal use provided that the source and the Institute's copyright notice are indicated.**

# Acknowledgements

I wish to thank all my acquaintances who have contributed to the success of this research work with their support and cooperation. This thesis appears in its current form with the assistance and guidance of many people. I would like to thank all of them for their kind support.

I would like to express my sincere gratitude to my supervisor, Assistant Professor Jac Fredo AR, for providing me with this research opportunity. Under his supervision, guidance, motivation, and support, I could be able to complete this work. His suggestions helped me to improve the quality of my work.

I sincerely thank my research progress evaluation committee members, Dr. Deepesh Kumar and Prof. M.S. Muthu. Their valuable suggestions, comments, and consistent support improved the quality of the research work. I gratefully acknowledge All the faculty and staff members of the school for their kind help whenever I needed it.

Additionally, I am immensely thankful for my esteemed labmates, including Abirami S, Praveen Kumar G, Chetan Tanaji Rakshe, Pragya, Ravi Ratnaik, Tikaram, Nour AL Shawa, B Vinay Kumar, Siddartha, and Abdul Aleem, whose collaborative efforts and friendship enriched this journey.

Moreover, I wish to thank my dear friends, E Suresh Kumar, Ch Anjaneyulu, and N Ome, who provided invaluable financial assistance during challenging times. Their generosity eased my burden and allowed me to focus on my academic pursuits.

---

I am also deeply indebted to my father, Shri. Shankar, mother, Mrs. Laxmi, family members, my brother Sridhar Kumar, and sister Sriveni, thank you for your unwavering support and encouragement at every step of this journey.

Last but certainly not least, I am profoundly grateful to my life partner, Mamatha, and our children, Balaji JayaKrishna and Durga Sri, for their boundless love, unwavering encouragement, unshakeable trust, and unwavering support. Their presence has been my pillar of strength, motivating me to persevere and succeed.

**SRIRAM KUMAR P**

# Abstract

**Keywords:** Emotion, Emotion recognition, Electrodermal activity, Decomposition, Segmentation, Windowing, Temporal features, Time-frequency representation, Time-encoded images, Machine learning

Emotions are fundamental aspects of human life that influence our thoughts, behaviors, and interactions with the world around us. Recognizing and understanding emotions is crucial in various aspects of life, including interpersonal relationships, mental health, and decision-making processes. Emotion detection holds significant importance in fields such as psychology, healthcare, and human-computer interaction. There are several ways to detect emotions, from traditional methods like facial expressions and vocal intonations to physiological signals such as Electrodermal Activity (EDA). It reflects changes in the skin's electrical conductance in response to emotional stimuli.

The EDA consists of several components, including tonic and phasic signals, which are influenced by the sympathetic nervous system activity associated with emotional states. For instance, variations in tonic signals may indicate overall arousal levels, while phasic signals represent rapid changes in arousal in response to specific stimuli. It is essential to understand the influence of EDA components, such as tonic and phasic signals for effective emotion detection. EDA signals are often complex and noisy, making it challenging to extract meaningful information. Segmenting the EDA signal into smaller, more manageable segments allows for targeted analysis of specific emotional responses. Hence, it is necessary to identify the significant segments of EDA signals to enhance emotion detec-

---

tion. Another important consideration is the windowing approach for EDA signals. Windowing involves dividing the continuous EDA signal into overlapping or non-overlapping windows for analysis. For instance, overlapping windows may capture temporal dynamics more effectively, while non-overlapping windows offer simpler processing but may miss transient emotional responses. The choice of windowing technique can significantly impact the effectiveness of emotion recognition algorithms. In this study, we attempted to identify the optimal component of the EDA signal and decomposition method, segment, and windowing approach using advanced signal processing methods and machine learning algorithms.

Initially, we obtained EDA signals from the publicly available Continuously Annotated Signals of Emotion (CASE) dataset for a 4-class categorical emotional classification. These signals underwent pre-processing, including applying a Butterworth low-pass filter with a 2 Hz cutoff frequency. We conducted three analyses to optimize EDA component and decomposition method, segment, and windowing approach as follows:

- 1) We employed convex optimization and Bayesian EDA decomposition methods to separate EDA signals into tonic and phasic components, then extracted ten temporal features from each component.

- 2) We considered the First-half, Second-half, and Whole phasic signals, generating spectrograms using the Short-Time Fourier Transform and Mel Frequency Cepstrum on considered signals. Features like Gray Level Co-occurrence Matrix (GLCM) and Gray Level Run Length Matrix (GLRLM) were extracted from these spectrograms.

- 3) We applied five and nine windows approaches with 50% overlapping on the Second half of the phasic signals. Then, each window of the time series signal was transformed into time-encoded images using the Gramian Angular Summation method, Gramian Angular Difference method, Markov Transition Field, and Recurrence Plot. From these images, we extracted features, including GLCM, GLRLM, fractal dimension texture analysis, Zernike's moments, Hu's moments, and first-order statistics.

---

Finally, we selected only the most significant features ( $p < 0.05$ ) of respective analyses obtained through the Kruskal-Wallis test. We applied these features independently to the three machine learning models, such as Support Vector Machine (SVM), Random Forest (RF), and XGBoost (XGB), to optimize the EDA components and decomposition method, segment and windowing approach.

Our findings revealed that phasic signals of EDA contributed well to emotion detection compared to the tonic component. The phasic signals decomposed by the cvxEDA decomposition method significantly impacted emotional state classification compared to the BayesianEDA method. We achieved an impressive accuracy of 86.87% with XGB, showcasing the method's efficacy in capturing relevant signals for emotion detection. Further, the Second half of the phasic signals contribute more information to emotion detection than the First half and Whole phasic signals. We achieved a remarkable classification accuracy of 97.08% with the SVM classifier. Finally, the nine windows of the Second half of phasic signals significantly improved emotion detection compared to the five-windows approach. We achieved a comparable accuracy of 88.24% using XGB. Our results underscore the importance of optimizing the EDA components, decomposition method, segments, and windowing approach to refine the emotion recognition systems and enhance classification performance.

The findings of this study offer substantial potential for a wide range of applications. These include healthcare monitoring systems, human-computer interaction interfaces, education and learning platforms, stress management and wellness mobile applications, virtual reality and augmented reality experiences, and the automotive and transportation industry. By integrating our advanced emotion recognition system, these applications can be significantly enhanced, leading to improved user experiences, greater well-being, and increased innovation across various industries.

# Contents

<b>1</b>	<b>Introduction</b>	<b>1</b>
1.1	Emotion	1
1.2	Emotion Paradigms	2
1.3	Emotion Recognition	3
1.4	Electrodermal activity	5
1.4.1	Background	5
1.4.2	Skin Anatomy	5
1.4.3	Electrodermal activity	6
1.4.4	EDA Recording	7
1.4.5	EDA Components	7
1.5	Decomposition of EDA: Tonic and Phasic	8
1.6	Importance of Feature Extraction in Emotion Recognition	10
1.7	Machine Learning in Emotion Recognition	12
<b>2</b>	<b>Literature Review</b>	<b>14</b>
2.1	Motivation	38
2.2	Objectives	38
<b>3</b>	<b>Materials and Methodology</b>	<b>40</b>
3.1	Process Pipeline	40
3.2	Dataset	44
3.2.1	Participant Information	44

3.2.2 Ethical Framework and Institutional Approval	44
3.2.3 Stimuli Information	44
3.2.4 Experimental Protocol	45
3.2.5 EDA Signal Description	45
3.3 Pre-processing	46
3.4 Decomposition Methods	47
3.4.1 Convex Optimization to EDA	47
3.4.2 Bayesian EDA	49
3.5 Time-Frequency Representation	51
3.5.1 Short Time Fourier Transform	51
3.5.2 Mel Frequency Cepstrum	52
3.6 Time-series to Image Generation	52
3.6.1 Gramian Angular Field	52
3.6.2 Markov Transition Field	54
3.6.3 Recurrence Plot	56
3.7 Feature Extraction	57
3.7.1 Temporal Features	57
3.7.2 Image based Features	59
3.8 Significance Test	60
3.9 Machine learning	61
3.9.1 Support Vector Machine	61
3.9.2 Random Forest	61
3.9.3 Extreme Gradient Boosting	62
<b>4 Results</b>	<b>66</b>
4.1 Representative of EDA Signals and their Analysis	67
4.2 Optimization of EDA and Decomposition Methods	71
4.2.1 Statistical Significance of temporal Features	73
4.2.2 Classification Results for Optimization of EDA and Decomposition Methods	77

---

<b>4.3 Optimization of Phasic Segments</b> . . . . .	81
<b>4.3.1 Statistical Significance of GLCM and GLRLM Features</b> . . . . .	82
<b>4.3.2 Classification Results for the Optimization of Phasic Segments</b> . . . . .	85
<b>4.4 Optimization of windowing approach</b> . . . . .	90
<b>4.4.1 Statistical Significance of GLCM, GLRLM, FDTA, FOS, HM,</b> <b>and ZM Features</b> . . . . .	91
<b>4.4.2 Classification Results for the Optimization of Windowing Approach</b>	97
<b>5 Discussions</b>	<b>107</b>
<b>5.1 Effect of Decomposition Methods</b> . . . . .	108
<b>5.2 Effect of Phasic EDA Segments</b> . . . . .	110
<b>5.3 Effect of Segment Windows</b> . . . . .	113
<b>5.4 Effect of Process-Pipeline</b> . . . . .	116
<b>6 Limitations and Future Directions</b>	<b>120</b>
<b>7 Conclusions</b>	<b>123</b>

# List of Figures

1.1	2D Russel circumplex emotional model	3
1.2	Anatomy of the eccrine sweat gland in various layers of skin	6
1.3	Electrode placements for recording EDA	8
1.4	Raw EDA and tonic and phasic components of EDA signal	9
3.1	Proposed process pipeline for this study	42
3.2	Representative segmented signals	43
3.3	Representative signal with (a) 5 windows and (b) 9 windows	43
3.4	Experimental setup of the CASE dataset	46
4.1	Representative EDA signals of a random subject's emotion: (a) raw signal and (b) low-pass filtered with a 2Hz cut-off frequency	67
4.2	Representative EDA signals of four random subjects for the same emotional state (a, c, e, g) before normalization and (b, d, f, h) after normalization	69
4.3	Representative EDA signals of various emotional states amusing, boring, relaxing, and scary: (a, c, e, g) before normalization and (b, d, f, h) after normalization	70
4.4	The representative signals of the amusing, boring, relaxing, and scary emotional states of a random subject (a, d, g, j) EDA, along with their corresponding decomposed components by the cvxEDA decomposition method (b, e, h, k) tonic and (c, f, i, l) phasic signals	72

4.5	The representative signals of the amusing, boring, relaxing, and scary emotional states of a random subject (a, d, g, j) EDA, along with their corresponding decomposed components by the BayesianEDA decomposition method (b, e, h, k) tonic and (c, f, i, l) phasic signals. . . . .	73
4.6	Representative box plots illustrating features extracted from cvxEDA phasic signal: (a) MFD, (b) MSD, (c) MAP, (d) STD, (e) DR, (f) MN, (g) MIP, and (h) MDN. . . . .	76
4.7	Representative box plots illustrating top eight significant features extracted from BayesianEDA phasic signal (a) MFD, (b) SFD, (c) SSD, (d) MSD, (e) MN, (f) MIP, (g) MAP, and (h) MDN. . . . .	78
4.8	Spectrogram representation of Scary emotion: comparison of STFT and MFC for First-half, Second-half, and Whole phasic signals. (a) First-half phasic signal with corresponding (d) STFT and (g) MFC spectrograms. (b) Second-half phasic signal with corresponding (e) STFT and (h) MFC spectrograms. (c) Whole Phasic Signal with corresponding (f) STFT and (i) MFC spectrograms. . . . .	81
4.9	Spectrogram representation of Boring emotion: comparison of STFT and MFC for First-half, Second-half, and Whole phasic signals. (a) First-half phasic signal with corresponding (d) STFT and (g) MFC spectrograms. (b) Second-half phasic signal with corresponding (e) STFT and (h) MFC spectrograms. (c) Whole Phasic Signal with corresponding (f) STFT and (i) MFC spectrograms. . . . .	82
4.10	Representative box plots of top eight significant features extracted from STFT: (a) SRE, (b) MMCC, (c) MIMC1, (d) RASM, (e) RCN, (f) Homogeneity, (g) Dissimilarity, and (h) Correlation. . . . .	86
4.11	Representative box plots of top eight significant features extracted from MFC: (a) MMCC, (b) RMCC, (c) MIMC1, (d) RIMC1, (e) RLU, (f) SRE (g) Homogeneity, and (h) RASM. . . . .	87

4.12	Representative (a) Low, (b) Medium, and (c) High fluctuations window signals and corresponding time-encoded images representation (d, e, f) GADF, (g, h, i) GASF, (j, k, l) MTF, and (m, n, o) RP . . . . .	92
4.13	Representative box plots of top eight significant features extracted from GADF: (a) RASM, (b) MIMC2, (c) RMIC2, (d) MIMC1, (e) MMCC, (f) RIMC1, (g) RMCC, and (h) MIDM. . . . .	98
4.14	Representative box plots of top eight significant features extracted from GASF: (a) MIDM, (b) Homogeneity, (c) RIDM, (d) MDV, (e) MDE, (f) RE, (g) RDV, and (h) RDE. . . . .	99
4.15	Representative box plots of top eight significant features extracted from MTF: (a) FOSSKW, (b) MDV, (c) RDV, (d) MIMC1, (e) MDE, (f) RSA, (g) Mean, and (h) MSA. . . . .	100
4.16	Representative box plots of top eight significant features extracted from RP: (a) RMCC, (b) MMCC, (c) RSE, (d) SRE, (e) MDV, (f) RLU, (g) RDV, and (h) Homogeneity. . . . .	101
5.1	Radar diagram representation for the optimization of signals and decomposition methods using performance metrics (a) Accuracy, and (b) F1-score. . . . .	110
5.2	Bar diagram representation for the optimization of phasic segments using performance metrics: (a) Accuracy, and (b) F1-score. . . . .	111
5.3	Bar diagram representation for the optimization of windowing approach using performance metrics: (a) Accuracy, and (b) F1-score. . . . .	114

# List of Tables

3.1	Description of CASE dataset	46
3.2	Comprehensive list of the features obtained from GLCM, GLRLM, FDTA, ZM, HM, and FOS.	64
3.3	Classifier hyperparameters and values.	65
3.4	Performance metrics for classifiers and formulas.	65
4.1	Statistical significance of features extracted from EDA, cvxEDA tonic, cvxEDA phasic, BayesianEDA tonic, and BayesianEDA phasic signals.	75
4.2	Classification results of SVM, RF, and XGB using temporal features extracted from EDA signals for four-class emotions.	77
4.3	Classification results of SVM, RF, and XGB using temporal features extracted from tonic and phasic signals obtained by cvxEDA decomposition method for four-class emotions.	79
4.4	Classification results of SVM, RF, and XGB using temporal features extracted from tonic and phasic signals obtained by BayesianEDA decomposition method for four-class emotions.	80
4.5	KW test for GLCM and GLRLM features extracted from STFT and MFC spectrograms for First-half, Second-half, and Whole phasic segments.	84
4.6	Classification results of SVM, RF, and XGB using First-half, Second-half and Whole phasic STFT.	88
4.7	Classification results of SVM, RF, and XGB using First-half phasic, Second-half, and Whole phasic for MFC.	89

---

4.8	Significance of features using KW test: GADF, GASF, MTF, and RP across 5 and 9 window approaches	93
4.9	Classification results of SVM, RF, and XGB using GADF images for five- window and nine-window approaches	102
4.10	SVM, RF, and XGB classification results using GASF images for five- window and nine-window approaches	103
4.11	SVM, RF, and XGB classification results using MTF images for five- window and nine-window approaches	105
4.12	Classification results of SVM, RF, and XGB using RP images for five- window and nine-window approaches	106
5.1	Summary of various frameworks for the classification of emotions using the CASE dataset	118
5.2	Summary of various frameworks for classifying emotions using the CASE dataset	119

# List of Abbreviations

**2D:** Two-dimensional

**3D:** Three-dimensional

**ANS:** Autonomic Nervous System

**ASM:** Angular Second Moment

**AUC:** Area Under the Curve

**AV:** Audio-visual

**BVP:** Blood Volume Pulse

**CASE:** Continuously Annotated Signals of Emotion

**CDA:** Continuous Decomposition Analysis

**CNN:** Convolutional Neural Networks

**CNS:** Central Nervous System

**CWD:** Choi–Williams Distribution

**cvxEDA:** Convex Optimization based on EDA

**CWT:** Continuous Wavelet Transform

- DDA:** Discrete Decomposition Analysis
- DCM:** Dynamic Causal Modeling
- DR:** Dynamic Range
- ECG:** Electrocardiogram
- EDA:** Electrodermal Activity
- EEG:** Electroencephalogram
- EMG:** Electromyogram
- ER:** Emotion Recognition
- FDTA:** Fractal Dimension Texture Analysis
- FOS:** First-Order Statistics
- GADF:** Gramian Angular Difference Field
- GAF:** Gramian Angular Field
- GASF:** Gramian Angular Summation Field
- GLCM:** Gray Level Co-occurrence Matrix
- GLRLM:** Gray Level Run-Length Matrix
- GLU:** Gray-Level Uniformity
- HM:** Hu's Moments
- HR:** Heart Rate
- HRV:** Heart Rate Variability
- HVHA:** High Valence/High Arousal

**HVLA:** High Valence/Low Arousal

**KNN:** K-Nearest Neighbors

**KW:** Kruskal-Wallis

**LR:** Logistic Regression

**LRE:** Long Run Emphasis

**LTI:** Linear Time-Invariant

**LVHA:** Low Valence/High Arousal

**LVLA:** Low Valence/Low Arousal

**MAP:** Maximum Peak

**MASM:** Mean of Angular Second Moment

**MCN:** Mean of Contrast

**MCR:** Mean of Correlation

**MDE:** Mean of Difference Entropy

**MDN:** Median

**MDV:** Mean of Difference Variance

**ME:** Mean of Entropy

**MFD:** Mean of First Derivative

**MFCC:** Mel-Frequency Cepstral Coefficients

**MFC:** Mel-Frequency Cepstrum

**MIDM:** Mean of Inverse Difference Moment

**MIMC1:** Mean of Information Measures of Correlation-1

**MIMC2:** Mean of Information Measures of Correlation-2

**MIP:** Minimum Peak

**ML:** Machine Learning

**MN:** Mean

**MMCC:** Mean of Maximal Correlation Coefficient

**MSA:** Mean of Sum Average

**MSD:** Mean of Second Derivative

**MSE:** Mean of Sum Entropy

**MSV:** Mean of Sum Variance

**MSSV:** Mean of Sum of Squares Variance

**MTF:** Markov Transition Field

**PNS:** Peripheral Nervous System

**RASM:** Range of Angular Second Moment

**RCN:** Range of Contrast

**RCR:** Range of Correlation

**RDE:** Range of Difference Entropy

**RDV:** Range of Difference Variance

**RE:** Range of Entropy

**RIDM:** Range of Inverse Difference Moment

**RIMC1:** Range of Information Measures of Correlation-1

**RIMC2:** Range of Information Measures of Correlation-2

**RLU:** Run Length Uniformity

**RMCC:** Range of Maximal Correlation Coefficient

**RPC:** Run Percentage

**RP:** Recurrence Plot

**RSA:** Range of Sum Average

**RSE:** Range of Sum Entropy

**RSP:** Respiration

**RSV:** Range of Sum Variance

**RSSV:** Range of Sum of Squares Variance

**SAM:** Self-Assessment Manikin

**SFD:** Standard Deviation of First Derivative

**SKT:** Skin Temperature

**SparsEDA:** Nonnegative Sparse Deconvolution

**SRE:** Short Run Emphasis

**SSD:** Standard Deviation of Second Derivative

**SS:** Sum of Squares

**STD:** Standard Deviation

**STFT:** Short Time Fourier Transform

**SVM:** Support Vector Machine

**TFR:** Time-Frequency Representation

**VA:** Valence-Arousal

**WVD:** Wigner–Ville Distribution

**XGB:** XGBoost

**ZM:** Zernike’s Moments

# List of Symbols

$A$  : State transition matrix

$B$  : Tall matrix containing cubic B-spline basis functions as columns

$C$  : Observation matrix

$C_P$  : Coefficient matrix for the phasic component

$C_T$  : Coefficient matrix for the tonic component

$T(t)$  : Diffusion/reabsorption

$D_{ij}$  : Euclidean distance between any two points in the phase space

$f$  : Frequency

$f$  : Linear frequency

$f_m$  : Mel-frequency

$H$  : Matrix representation in the Laplace transform of  $h(t)$

$H_m(f_k)$  : Value of the m-th triangular filter at frequency  $f_k$

$h(t)$  : Impulse response shaped as a bi-exponential Bateman function

$I$  : Current

$j$  : Imaginary unit

$l$  : Vector of spline coefficients

$M$  : Tridiagonal matrix with moving average coefficients

$M_{ij}$  : Element of the MTF matrix representing the transition probability based on the time order of the original time series

$P(t)$  : Phasic component

$p$  : Sudo Motor Nerve Activity (SMNA)

$q$  : Auxiliary variable

$q$  : Vector in optimization problems

$q(x_i)$  : Bin to which the value  $x_i$  belongs

$R$  : Recurrence matrix

$R$  : Skin resistance

$r$  : Phasic activity

$ri$  : Radius in polar coordinates

$S(t)$  : Sweat secretion via pore opening

$S(f_k, t)$  : Spectrogram magnitude at frequency  $f_k$  and time  $t$

$SC(t)$  : Skin conductance at time  $t$

$SC_P(t)$  : Phasic component of skin conductance at time  $t$

$SC_T(t)$  : Tonic component of skin conductance at time  $t$

$t$  : Tonic component

$\tau$  : Delay coefficient in phase space reconstruction

$\tau$  : Variable representing time in STFT

$\tau_1$  : Slow time constant of the phasic curve shape

$\tau_2$  : Fast time constant of the phasic curve shape

$u(t)$  : Unitary step function

$u_k$  : Input at discrete time step  $k$

$U$  : Heaviside step function

$V$  : Voltage

$W$  : Markov transition matrix

$w(t - \tau)$  : Window function in STFT

$w_{ij}$  : Probability of transitioning from bin  $i$  to bin  $j$

$X$  : Original time series data

$X$  : Time series data

$X(t)$  : Time series data

$\hat{X}$  : Normalized time series

$x(t)$  : Time-domain signal

$x_k$  : State variable at discrete time step  $k$

$\epsilon$  : Additive independent and identically distributed zero-average Gaussian noise term

$\epsilon$  : Threshold distance in phase space reconstruction

$\mu S$  : MicroSiemens

$\phi$  : Angle

$\phi_i$  : Polar angle corresponding to the  $i$ -th element of the time series

$\nu(t)$  : Observation noise at time  $t$

$\nu_k$  : Observation noise at discrete time step  $k$